THE JOURNAL OF PHYSICAL CHEMISTRY C

C: Surfaces, Interfaces, Porous Materials, and Catalysis

An Unsuitable Li-O2 Battery Electrolyte Made Suitable with the Use of Redox Mediators

J. Padmanabhan Vivek, Tom Homewood, and Nuria Garcia-Araez

J. Phys. Chem. C, **Just Accepted Manuscript** • DOI: 10.1021/acs.jpcc.9b03403 • Publication Date (Web): 15 Jul 2019

An Unsuitable Li-O_2 Battery Electrolyte Made Suitable with the Use of Redox Mediators

J. Padmanabhan Vivek, Tom Homewood, Nuria Garcia-Araez**

Chemistry, University of Southampton, Highfield Campus, SO17 1BJ, UK

ABSTRACT. The unique properties of room temperature ionic liquids make them promising electrolytes for next-generation rechargeable batteries. Unfortunately, many promising ionic liquid electrolytes suffer degradation under the operation conditions of Li-O_2 batteries. This work demonstrates that the addition of redox mediators can transform the reaction mechanism and suppress the degradation of the electrolytes in Li-O_2 batteries. 1-ethyl-3-methylimidazolium bis(trifluoro-methylsulfonyl)imide (EMIMTFSI) is a room temperature ionic liquid that is widely being explored for battery applications, but its instability in the presence of reduced oxygen species (superoxide) limits application in Li-O_2 batteries. The addition of redox mediators can suppress the degradation of EMIMTFSI in Li-O_2 cells, leading to remarkable improvements in capacity and reversibility. In-situ Surface Enhanced Raman Spectroscopy and operando-pressure evaluation demonstrate that 2,5-di-tert-butyl-1,4-benzoquinone (DBBQ) is capable of suppressing the attack of superoxide species against EMIMTFSI, thus promoting the desirable 2-electron pathway to Li_2O_2 discharge product. A detailed evaluation of the gas evolution was carried out using online mass spectrometry. In spite of an efficient 2-electron oxygen reduction with the use of DBBQ additive, this effect did not translate into a substantial improvement in the

oxygen evolution during charging. However, when a charge mediator was used in combination with DBBQ, a significant improvement in oxygen evolution could be observed. This work provides the first direct experimental evidence that redox mediators can enable the incorporation of electrolytes prone to degradation by the attack of superoxide species in practical and reversible Li-O_2 batteries.

1. Introduction

The reversible electrochemistry between molecular oxygen and lithium in aprotic electrolytes has undergone extensive scrutiny in recent years as it holds promise to a high energy battery technology.[1,2,11,3–10] The theoretical specific energy of the Li-O_2 battery surpasses any current battery technology, and some encouraging early reports endorsed non-aqueous Li-O_2 battery as a promising next-generation energy storage technology.[12,13,22,14–21] Of the many fundamental challenges, the development of electrolytes with chemical resistance against the attack of oxygen reduction products (e.g. superoxide,[23,24] singlet oxygen[25,26]) and capable of impeding the cathode passivation problem (resulting from deposition of the Li_2O_2 discharge product) is arguably the most crucial one.[27–29] The use of high donor number solvents and the addition of redox mediators to the electrolyte have been found to circumvent the electrode passivation problem thus improving the storage capacity.[30–39] High donor number solvents tend to be less stable against oxygen reduction products; hence, the use of redox mediators seems more promising. Generally, redox mediators are used in Li-O_2 batteries to mediate the oxygen electrode reactions by transporting electrons from the electrode to oxygen (during cell discharge) or from the discharge products to the electrode (during charging) thus improving electron transfer kinetics whilst encouraging the formation of discharge products away from the electrode surface. Consequently, an efficient redox mediation improves performance indexes such as storage capacity, voltage gap and cycle life. A few recent fundamental studies also suggest that the lifetime of oxygen reduced species (e.g. superoxide) is significantly reduced in the presence of discharge mediators thus reducing their parasitic reactivity.[40,41] The effect of redox mediation on the electrolyte stability and discharge/charge efficiency is evaluated in this study, showing how an unsuitable electrolyte

for Li-O_2 applications, due to its instability and degradation in the presence of oxygen reduced species, becomes stable and resistant to degradation in the presence of redox mediators.

Room temperature ionic liquids are particularly attractive as battery electrolytes because of their wide potential window, low flammability, low vapor pressure and high thermal stability.[42–46] Even though 1-ethyl-3-methylimidazolium bis(trifluoro-methylsulfonyl)imide (EMIMTFSI, see structure in Figure 1) was initially considered as a prospective electrolyte for Li-O_2 batteries, later it was found that the imidazolium cation is unstable against superoxide radicals.[47,48] Using molecular orbital calculations, it has been shown that superoxide can attack the C-2 of the imidazolium cation to form an ion pair complex first [47,49,50] then abstract the proton attached to the C-2 (see Figure S12), and with this triggering the degradation of imidazolium cation, generating hydrogenated superoxide and peroxide species alongside.[47] This is very unfortunate since EMIMTFSI is a promising ionic liquid for batteries because of its advantageous properties such as relatively low viscosity and good ionic conductivity.[51–53] Furthermore, due to their negligible vapor pressure, general strategies to suppress the degradation of ionic liquids are crucial for the development of a breathing Li-air battery technology where O_2 could be fed from air, thus enabling a very light battery at a system level. Bruce's group recently reported the use of 2,5-di-tert-butyl-1,4-benzoquinone (DBBQ, see structure in Figure 1) as a mediator for nonaqueous Li-O_2 batteries.[54] Unlike other discharge mediators explored so far, the Li-O_2 discharge reaction in the presence of DBBQ has been proposed to proceed via a unique pathway that avoids the formation of 'free' superoxide in solution. A complex between the reduced DBBQ species and oxygen (LiDBBQO_2) has been proposed to be the main intermediate reaction product in the Li-O_2 discharge reaction, thus replacing and bypassing the formation of

superoxide (LiO_2) as the reaction intermediate. This proposed mechanistic pathway suggests that DBBQ can be particularly effective in promoting the stability of the electrolyte.

In this work, the incorporation of DBBQ redox mediator to an EMIMTFSI electrolyte in Li-O_2 batteries is investigated, for the first time, with the purpose of enabling an alternative discharge reaction mechanism in which the degradation of the EMIM cation by the attack by superoxide is overcome. Operando analytical techniques are employed to investigate the absence of degradation reactions. Operando pressure measurements are used to quantify the amount of oxygen consumed during discharge, and operando electrochemical mass spectrometry is applied to quantify the amount of oxygen evolved during charge. In-situ Raman measurements are applied to study the discharge reaction mechanism. In addition, the incorporation of a charge mediator (lithium iodide), combined with the DBBQ discharge mediator is shown to produce drastic improvements in the oxygen reduction/evolution efficiency. The approach here proposed is expected to be applicable to other electrolytes, thus opening a new route that could enable the implementation of so far considered "unsuitable" electrolytes (due to severe degradation problems) to Li-O_2 batteries.

2. Experimental

Materials, cell assembly and instrumentation

The electrolyte preparation and the cell assembly were carried out in an argon filled glovebox (<1 ppm O_2, <1 ppm H_2O). 1-ethyl-3-methylimidazolium bis(trifluoromethylsulfonyl)-imide (99.9%,) was purchased from Solvionic and dried under vacuum at 120 °C for 18 hours under constant stirring, then the sealed container is transferred to the glove box. Hi-Dry® bis(2-Methoxyethyl) Ether solvent (DG, >99.8%, Water <20 ppm) was purchased from ROMIL Ltd. and further dried over molecular sieves at room temperature. The salts bis(trifluoro-methylsulfonyl)imide lithium salt (99.95%, Sigma-Aldrich) and lithium iodide (99.999%, Sigma-Aldrich) were dried under vacuum at 120 °C for 48 hours. 2,5-di-tert-butyl-1,4-benzoquinone (99%, Sigma-Aldrich) and Celgard® separator were dried under vacuum at 40°C, and Quintech H23® gas diffusion layer at 80°C under vacuum for one week. Pelletized Li_2O-Al_2O_3-SiO_2-P_2O_5-TiO_2-GeO_2 lithium ion conducting glass ceramic (LICGC) of 1 inch diameter and 150 μM thick was purchased from Ohara GmbH and used as received. Swagelok and SERS cell components and LICGC were dried under vacuum at 80 °C for 12 hours and directly transferred to the glovebox. All salts were transferred to the glovebox in sealed Buchi® glass tubes, and the electrolytes were prepared and cells assembled inside the same glovebox(<1ppm O_2, <1ppm H_2O). Both SERS electrochemical cell and the Swagelok type cell were purged with dry oxygen (BOC N5.0 O_2).

Biologic's VMP multichannel potentiostat/galvanostat was used for all electrochemical measurements, except for the electrochemical SERS, in which an Autolab PGSTAT101 potentiostat/galvanostat was used. A 1-inch Swagelok-type symmetrical cell made of stainless steel was used for galvanostatic cycling. The cell was equipped with a steel plunger to allow the

cell to be purged with dry oxygen. Cell design and assembly: The cell used throughout this study is of symmetrical (2-electrode) type equipped with 1 inch Swagelok steel straight union body and steel current collectors on either side. The cell stack follows this order: Anode current collector, lithium anode (1" diameter), Celgard 24001 separator, LICGC separator, Celgard 24001 separator, Quintech H23 cathode (1" diameter), stainless steel mesh spacer, stainless piston with flow-through holes, then a stainless steel gas flow plunger equipped with gas inlet and outlet valves. The inside of the stainless steel cell body was electronically isolated from the cell stack using an insulating sheet of FEP (0.127 mm thick, RS components). The electrolyte on the lithium anode side consisted of 50 μL 1M LiTFSI/DG, and the Celgard separator used on this side of the LICGC was pre-wetted in this anolyte. The electrolyte on the cathode side consisted of 100 μL 1M LiTFSI/EMIMTFSI (containing the redox mediator(s) where applicable), and the Celgard separator used on this side of LICGC was also pre-wetted in the catholyte. LICGC used in between the Celgard separators separates the catholyte and anolyte so that the reaction of EMIMTFI or redox mediators with lithium metal is prevented.

Operando pressure measurements

The total amount of gases consumed and evolved during electrochemical cycling were determined by monitoring the internal pressure of the Swagelok type cell using a pressure transducer. The pressure transducer (PA-33X, Keller Druck AG) was attached to the Swagelok-type Li-O_2 cell using stainless steel gas pipes and compression fittings (Swagelok®). Oxygen purging though the transducer attached Swagelok type cell was done as follows: While the valves to the electrochemical cell were shut, the pressure transducer and the tubing attached to this were opened to vacuum for 20 minutes, then the valve was opened to dry oxygen. This sequence was repeated three times in order to remove any contaminants within the tubing or the

transducer. After this, the valve connected to the Swagelok cell was opened and allowed dry oxygen to flow through the cell-transducer assembly for 20 minutes. The cell-transducer assembly was sealed and isolated from the gas line, then allowed to rest inside a climatic chamber set to 25°C (HPP110, Memmert GmbH) for at least 2 hours so as to achieve thermal equilibrium. The internal pressure of the cell was monitored for 30 minutes prior to electrochemical cycling in order to ensure that the cell-transducer assembly is leak-free and the temperature is constant. The pressure change corresponding to gas consumed or evolved was converted to the number of moles of gas consumed or evolved, using the ideal gas law. During discharge, the gas consumed corresponds to oxygen consumption, since there is no other gas present in the cell. Once the pressure measurement is finished, the internal volume of the cell was determined using the known volume of the transducer and based on the pressure-volume relation (Boyle's law) upon equilibrating two interconnected vessels having unequal pressure. Once the volume is determined, the number of moles of gas consumed or evolved can be determined from the pressure difference observed, using the ideal gas law.

Operando electrochemical mass spectrometry (OEMS)

OEMS measurements were carried out using a quadrupole mass spectrometer (QGA, Hiden Analytical) equipped with an SEM ion detector. The spectrometer was configured for continuous analysis of gases, sampling at a specific sampling rate. The electrochemical cell used for OEMS was the same type as the ones used for pressure measurement, but without the transducer attached to the cell. The cells were discharged to their respective capacity values before connecting to the OEMS gas line. Nominally dry argon (BOC N5.0, <3ppm H_2O) flow at 0.8 ml/min (Bronkhorst Flow controller) flows through the gas flow system connected to the OEMS's inlet, this flow rate was chosen to match the OEMS's sampling rate. The flow system is

also equipped with a vacuum line that allows removal of contaminants from the additional tubing and fittings connecting the electrochemical cell to the gas line. The carrier gas argon was then allowed to flow through the electrochemical cell for 3 hours, allowing any remaining oxygen in the cell to be replaced by the carrier gas and to reach dynamic equilibrium with the electrolyte and the cell components. QGA records the gases analyzed in ppm; the amount of gas detected can be converted to mol/min knowing the flow rate of the carrier gas.

In-situ Surface-Enhanced Raman Spectroscopy (SERS)

In-situ SERS measurements were carried out by applying a reduction current of 0.02 mA/cm^2 on a sphere segment void plasmonic (SSV) gold working electrode. SERS spectra were recorded using a Renishaw Raman spectrometer at an excitation wavelength of 783 nm. A Leica microscope with a 50X objective lens was the collection optic. A background spectrum was collected at the open circuit potential then a reduction current of 0.02 mA/cm^2 (chronopotentiometry) was applied and spectra were collected in-situ every minute (30 seconds acquisition time) for 30 minutes.

The SSV substrate was prepared by template assisted electrodeposition method following the methodology reported elsewhere.[55] A gold coated glass microscope slide was used as the substrate for electrodeposition. The substrate was first cleaned by sonication in 2-propanol, followed by rinsing in deionized water and purging dry argon over the gold coated side for 10 minutes. The colloidal polystyrene template was prepared in a thin layer cell formed over this glass substrate by placing a cover glass over the gold coated side, keeping the two glass plates approximately 100 μm apart using a Parafilm® spacer. The as formed thin layer cell was filled with the colloidal polystyrene suspension and then allowed the solvent to evaporate slowly at 5°C inside a refrigerator. Once the solvent is completely dried out, the gold electrodeposition

was performed in a 3-electrode electrochemical cell at room temperature. A cyanide-free gold plating solution (ECF 60, Metalor) in combination with a plating additive (Brightener E3, Metalor) was the electrolyte used for gold deposition. The polystyrene coated gold substrate was the working electrode and a platinum mesh was used as the counter electrode. Electrode deposition was carried out by applying -0.72 V vs. saturated calomel reference electrode (SCE) until an estimated charge corresponding to the desired thickness of gold (for optimal SERS enhancement) has been passed through the polystyrene template. Further details on the SSV substrate preparation can be found elsewhere.[56] After electrodeposition, the as prepared SSV substrate was washed in ethanol, dried, then stored in DMF for several days in order to remove polystyrene nanospheres and insulating masks covering the gold substrate. A homemade three-electrode spectroelectrochemical cell made of PCTFE was used for in situ SERS measurements. The design of the cell with a quartz window on the top allows a thin layer of the electrolyte to sit on top of the SSV substrate working electrode and the Raman laser can then be focused onto this. The cell consists of SSV substrate working electrode, platinum wire counter electrode and a $Li_{0.5}FePO_4$ coated silver wire as the reference electrode. All cell components were dried at 80 °C in a vacuum oven for 12 hours then transferred straight to the glovebox. The SERS cell was assembled inside the glovebox, then dry oxygen was bubbled through the electrolyte in a small purging bottle attached to the SERS cell which then allows to transfer the oxygen-saturated electrolyte directly from the container to the thin layer SERS cell, without leaking oxygen to the glovebox atmosphere. The sealed SERS cell was then brought outside the glovebox to carry out the in-situ measurements.

X-Ray Diffraction (XRD)

A carbon-coated Celgard cathode made using a slurry containing 66.6 %wt. acetylene black and 33.3 %wt. lithiated Nafion (Ion power), was used for XRD characterization of the discharge products. After discharging the cell in pure O_2, the Swagelok type cell was transferred to the glovebox. The acetylene black based cathode was then hermetically sealed in an XRD holder (Bruker). The XRD was performed on a Rigaku Smartlab® with a Cu Kα source.

3. Results and Discussion

Electrochemistry

The Li-O_2 cell shows poor capacity when a 1 M LiTFSI/EMIMTFSI was used as the electrolyte (Figure 1, black curve), but the capacity improves significantly when the discharge mediator DBBQ is added to the electrolyte (Figure 1, red curve). The expected charge/cm^2 for a 1-electron reduction of all the DBBQ present in the cell would correspond to only 0.026 mAh/cm^2 (estimated based on the DBBQ concentration and volume of electrolyte). The higher capacity observed in the presence of DBBQ can be attributed to improved oxygen reduction reaction (ORR) kinetics and reduced electrode passivation in the presence of the DBBQ discharge mediator.[54] The maximum achievable capacity depends on several kinetic factors. Due to the competing unmediated reduction of oxygen to form Li_2O_2 at the electrode surface, surface passivation would eventually produce the end of discharge as the electrode surface is covered by the discharge product precipitates. The problem of the competing unmediated ORR is particularly important in ionic liquids, because their high viscosity slows down the diffusion of the redox mediator, and hence this limits the rate of the mediated ORR. On the contrary, the diffusion coefficient of oxygen in ionic liquids is relatively high,[57,58] which makes the effect of the unmediated ORR more prominent in ionic liquids compared to conventional electrolytes, thus resulting in lower capacities. Apart from these kinetic factors, the lower capacity observed

here also stems from the low porosity and low surface area of the commercial gas diffusion layer cathode (carbon cloth). As demonstrating a high achievable capacity is not the purpose of this study, we have chosen a commercial gas diffusion layer carbon cloth as cathode in this case. While the observed improvement in capacity upon the addition of DBBQ is promising, it is important to verify that the improved capacity is in fact a result of improved ORR kinetics and not related to any side reactions promoted by the mediator. Application of analytical techniques, as described below, is necessary to substantiate this.

In-situ Surface-Enhanced Raman Spectroscopy Analysis

In order to obtain a mechanistic understanding of the DBBQ-mediated ORR in the EMIMTFSI/LITFSI electrolyte, an in-situ Surface-Enhanced Raman Spectroscopy (SERS) analysis was carried out. A nanostructured gold electrode with sphere segments voids (SSV) served as the working electrode, instead of porous carbon cathode used in typical Li-O_2 cells. The SSV gold electrode used for SERS analysis serves as a model system to obtain mechanistic clues into the underlying processes. High surface sensitivity of the SERS technique helps to probe changes at the interfacial region. The SERS analysis presented here provides evidences for reduced surface passivation and suppressed parasitic reaction in the presence of DBBQ.

Upon application of a reduction current (0.02 mA/cm^2) to the SSV gold electrode in oxygen-saturated 0.1 M LiTFSI in EMIMTFSI electrolyte, a new Raman band appears at ca. 1616 cm^{-1} that grows in intensity over time (Figure 2a). This band can be attributed to degradation products that result from the attack of superoxide to the EMIM cations,[48] thus indicating the chemical instability and unsuitability of the EMIMTFSI ionic liquid for Li-O_2 battery applications. Remarkably, the spectra measured in the presence of DBBQ (Figure 2b) evidence quantitative suppression of degradation reactions, since the band at 1616 cm^{-1} is absent or suppressed. (Close

inspection of the spectra in DBBQ also shows a small band appearing in this region, which might indicate that some side reactions of EMIMTFSI happen even in the presence of DBBQ. If so, those minor side reactions might be prevented at higher DBBQ concentrations.)

The suppression of passivation issues is inferred from the behavior of the spectra in the 1300 – 1500 cm^{-1} region, where most of the bands are related to the ionic liquid cation (EMIM) itself (Table S2). The intensity of these bands (1300 – 1500 cm^{-1}) markedly increases with time during the application of an oxygen reduction current in the presence of DBBQ (Figure 2b), while the intensity of these bands remains relatively low without DBBQ (Figure 2a). This difference in the EMIMTFSI band intensities between the two cases is ascribed to surface passivation in the absence of a discharge mediator. Because of effective redox mediation in the presence of DBBQ, the surface is not immediately passivated by the discharge products, allowing to more clearly observe the change in EMIMTFSI bands at the interfacial region. The increasing band intensities in the 1300 cm^{-1} – 1500 cm^{-1} region in Figure 2b indicates that more EMIM cations (Table S2) are being partitioned to the interfacial region as the electrode is negatively polarized. Though these peaks corresponding to EMIM and TFSI are present in the absence of DBBQ as well (Figure 2a), the change in peak intensity with potential is relatively small, presumably due to the formation of a passivating Li_2O_2 layer on the electrode surface which affects the surface enhancement of the SSV gold substrate underneath.

The formation of reduced oxygen species is observed in the 1000 – 1200 cm^{-1} region in Figure 2, but EMIMTFSI also has several bands in the same region (Table S2) which complicates the assignment of the bands. In the absence of DBBQ, a band appears at 1105 cm^{-1} in Figure 2a during ORR (cyan region). At the open circuit potential, an small band corresponding to EMIMTFSI can be observed at 1088 cm^{-1}, but the 1105 cm^{-1} band evolved during ORR appears

distinct from this and increases in intensity with time, suggesting the accumulation of a reduced oxygen species corresponding to this band. Therefore, this band is tentatively assigned to weakly coordinated superoxide species; the relatively low O-O stretching band position is indicative of superoxide species coordinated to the ionic liquid cation rather than Li^+.[48,59] We also observe another band evolving around 805 – 810 cm^{-1} (cyan region in Figure 2a) during ORR which is indicative of Li_2O_2 formation. This peak is slightly blue-shifted for a Li_2O_2 band typically reported in the 790 – 805 cm^{-1}. In the presence of DBBQ, in addition to a 805 cm^{-1} peak, we observe a 835 cm^{-1} peak in Figure 2b. While the 805 cm^{-1} peak would indicate Li_2O_2-like species as in the previous case, the 835 cm^{-1} peak could be related to complexed peroxo species.[60] While the bands corresponding to Li_2O_2-like species appear in both cases (Figure 2a and 2b), a striking difference between the two is the observation of a rather strong peak at 1118 cm^{-1} when DBBQ is present in the electrolyte (Figure 2b). The presence of a 1118 cm^{-1} peak in Figure 2b would suggest that it is related to DBBQ-lithium-superoxo complex in 1M LiTFSI/EMIMTFSI electrolyte which might be present as a reaction intermediate species. However, a definitive assignment of this band is, unfortunately, not possible.

While the assignment of superoxide and peroxide bands observed here are complicated, our SERS analysis do provide two important observations: i) reduced surface passivation (as inferred from the potential-dependent change of band intensities in the 1300 – 1500 cm^{-1} region), and ii) the absence of the EMIM-degradation peak at 1616 cm^{-1} when DBBQ is present in the electrolyte. Because the SSV film was not stable enough at positive potentials, the SERS analyses were limited to discharge reactions only. Forthcoming sections of this article discuss the influence of redox mediators on the oxygen reduction and evolution efficiencies, evaluated using operando pressure measurements and operando electrochemical mass spectrometry (OEMS).

Operando Gas Consumption and Evolution Analyses

When a Li-O_2 cell using 1M LiTFSI/EMIMTFSI electrolyte was discharged at 0.02 mA/cm^2, the voltage dropped to 2 V vs. Li^+/Li in just about one hour, resulting in a capacity of 0.021 mAh/cm^2 (Figure 3a) and the gas consumption data indicates a reaction stoichiometry of 1.80 electrons per oxygen (Figure 3b). Gas consumption was estimated from the cell's internal pressure monitored in operando (original pressure data in the supplementary info, Figure S1). The observed deviation from an ideal 2-electron ORR suggests that the discharge reaction involved pathways/reactions other than the neat 2-electron conversion of O_2 into Li_2O_2. This deviation is mostly likely due to a fraction (~ 20% in this case) of the superoxide generated (1-electron ORR) being consumed for parasitic reactions other than the intended Li_2O_2 formation. After the cell discharge, the cell was allowed to relax for one hour and no appreciable pressure drop was observed during this time (Figure S1), demonstrating that the observed pressure drop is indeed due to gas consumption (specifically, oxygen consumption, since there is no other gas in the cell during the first discharge). The gas evolution upon charging (Figure 3b, red curve) deviates significantly from the 2-electron OER expected for an ideal Li_2O_2 to O_2 reaction. Because the gas evolution observed here doesn't necessarily indicate oxygen evolution alone, additional experiments were performance where operando electrochemical mass spectrometry (OEMS) was employed to identify the gaseous products formed in the charging process. The corresponding OEMS data (Figure 3c) shows that the amount (and rate) of oxygen evolved is indeed very low (for a 2e-/O_2, the expected rate is 30.5 mol/min). The oxygen recovery efficiency is estimated to be 11% (Table S3). The oxygen recovery efficiency is calculated as the ratio of the amount of oxygen evolved obtained from OEMS analysis (Figure 3c, red curve – oxygen) and the amount of oxygen consumed determined from the operando-pressure data

(Figure 3b, black curve). Significant CO_2 evolution was also observed as the potential rises above ~ 4 V vs. Li^+/Li. Clearly, the performance of a Li-O_2 cell containing 1M LiTFSI/EMIMTFSI is very poor; shows very low capacity, poor selectivity towards 2-electron ORR and the oxygen evolution efficiency is also very poor.

Figure 4 shows the electrochemical data and corresponding gas consumption/evolution in 1M LiTFSI/EMIMTFSI containing 50 mM DBBQ additive. The capacity was limited to 0.25 mAh/cm^2 (Figure 4a) in order to restrict the discharge curve to the voltage range where DBBQ actively mediates the discharge process. The oxygen consumption data (Figure 4b) shows a near-ideal 2-electron ORR in this case, and ex-situ XRD of the discharged electrodes confirms the formation of Li_2O_2 as the main discharge product (Figure S6). Unfortunately, the oxygen evolution is still very poor as evident from the gas evolution data (figure 4b, red curve). Though operando OEMS analysis suggests an improvement in the oxygen evolution rate in the presence of DBBQ (figure 4c, red curve), it is still significantly low compared to the desired 30.5 mol/min rate corresponding to full conversion of Li_2O_2 to O_2. The oxygen recovery efficiency is estimated to be 19%. As in the previous case, CO_2 evolution starts as the potential raises above ~ 4 V vs. Li^+/Li.

A poor oxygen evolution efficiency in spite of a near-ideal ORR reaction (in terms of electrons consumed per oxygen) might be a result of poor electronic contact of the discharge product with the electrode surface (an intrinsic consequence of discharge mediation). In order to efficiently oxidize discharge species that are not directly accessible to the electrode, iodide was added as a charge mediating additive to the electrolyte. While iodide is known to play complex roles in Li-O_2 batteries,[61–67] we have observed that incorporation of this charge mediator produced a significant improvement in oxygen evolution efficiency, in agreement with previous studies with

Li_2O_2-preloaded electrodes.[68] To complement this study, we have also looked into the effect of iodide in EMIMTFSI-LiTFSI in the absence of any discharge mediator (Figure S3) and, interestingly, in the absence of DBBQ, the oxygen recovery efficiency remained poor (15%) though iodide was present as a charge mediator.

Figure 5 shows that the oxygen consumption during ORR in the dual mediator electrolyte corresponds to a reaction stoichiometry of 2.34 electrons/O_2. Ex-situ XRD of the discharged electrodes confirms the formation of Li_2O_2 and LiOH discharge products. The deviation from 2-electron ORR due to the influence of iodide is lower when DBBQ is also present in the electrolyte (compare Figure S3b and Figure 5b). More interestingly, OEMS data shows significant improvement in oxygen evolution in the presence of the dual mediators and there is virtually no CO_2 evolution. The estimated oxygen recovery efficiency has improved to 56% with the use of dual mediators. Though iodide mediator helped to improve oxygen evolution, the use of iodide also promoted some LiOH formation during discharge. Consequently, the poor oxygen recovery efficiency could be related to the inefficiency in promoting LiOH oxidation by this mediator at these potentials. Nevertheless, the results obtained with the dual mediators clearly shows that the use of a charge mediator certainly improves the reversible oxygen evolution by efficiently mediating the oxidation of the discharge products formed via DBBQ mediation. Moreover, with the use of more efficient mediators, it is, in principle, possible to achieve near-ideal oxygen reduction/evolution in Li-O_2 cells containing 'otherwise unstable' electrolytes.

This work does not propose EMIMTFSI/LITFSI as a prospective electrolyte or DBBQ and LiI as ideal mediators for practical Li-O_2 batteries, but this evaluation points to the fact that a judicious choice of the mediators can widen the choice of suitable, chemically stable electrolytes for Li-O_2 battery applications. In fact, the use of dual mediators in Li-O_2 batteries has been

demonstrated by other groups in recent years,[69–72] but this work provides the first direct experimental evidence that redox mediators can enable the incorporation of electrolytes prone to degradation by attack by superoxide species in reversible Li-O_2 batteries. Discovering mediators that promote reaction pathways through less parasitic intermediates that lead to the desirable end products would be the key. Focusing on the discovery of efficient and stable redox mediators, and scrutinizing the true reversibility of the reactions with operando analytical techniques, is indeed a promising strategy to support the development of sustainable Li-O_2 batteries.

4. Summary

The effect of a discharge redox mediator DBBQ in LiTFSI/EMIMTFSI electrolyte in Li-O_2 batteries has been evaluated using in-situ surface enhanced Raman spectroscopy (SERS), operando pressure measurements and operando electrochemical mass spectrometry (OEMS). In-situ SERS analysis reveals improved stability of EMIMTFSI and reduced surface passivation in the presence of the discharge mediating DBBQ additive. The oxygen recovery efficiency of Li-O_2 cells were evaluated by combining operando pressure measurements with OEMS analysis. It is observed that DBBQ facilitates the ideal 2-electron reduction of oxygen, forming Li_2O_2, but the efficiency of oxygen evolution was poor when no charge mediator was used. The use of iodide charge redox mediator, combined with DBBQ discharged mediator, resulted in significant improvement in the oxygen recovery efficiency. In conclusion, this work demonstrates that redox mediators can selectively promote the desired reactions of oxygen reduction and evolution in Li-O_2 cells and simultaneously suppress the degradation of the electrolyte, thus enabling the use of advantageous electrolytes such as EMIMTFSI, which are otherwise unacceptable for practical Li-O_2 batteries.

Supporting Information.

Galvanostatic cycling data, corresponding gas consumption/evolution analysis and OEMS analysis of Li-O_2 cells with 1 M LiTFSI/EMIMTFSI electrolyte and 50 mM iodide additive.

Original operando pressure data and OEMS data corresponding to all gas consumption/evolution analyses and OEMS analyses presented in this article.

XRD analysis of the discharged electrodes compared to a pristine electrode.

Electrochemical data corresponding to SERS analysis

Raman spectra of EMIMTFSI and DBBQ and a table detailing the band assignments for EMIMTFSI

Chemical structure of EMIMTFSI and DBBQ

Conductivity studies of the electrolyte

OEMS background spectra

Table comparing the effect of mediators on the oxygen recovery efficiency.

AUTHOR INFORMATION

Corresponding Authors

* vjp1v16@soton.ac.uk (J. Padmanabhan Vivek), n.garcia-araez@soton.ac.uk (Nuria Garcia-Araez)

Author Contributions

J. Padmanabhan Vivek performed most of the experiments reported here and Tom Homewood contributed with the XRD characterization and preliminary electrochemical characterization. J. Padmanabhan Vivek produced the first draft of the article and all authors contributed to the discussion and production of the final version of the article. Nuria Garcia-Araez supervised the project.

ACKNOWLEDGMENTS

Funding Sources**:** EPSRC (EP/N024303/1), FP7-MC-CIG FunLAB project (630162), Royal Society Research Grant (RG130523).

EPSRC is gratefully acknowledged for financial support though an early-career fellowship awarded to N. Garcia-Araez (EP/N024303/1). Financial support from the European Commission through the FP7-MC-CIG FunLAB project (630162) and from the Royal Society for a Research Grant (RG130523) is also gratefully acknowledged. The authors would also like to thank Prof. Andrea E. Russell for providing generous access to the in-situ Raman facility and Mr. Alex Keleer and Dr. James T. Frith for support with the training in the Raman electrode substrate preparation and the Raman measurements.

FIGURES

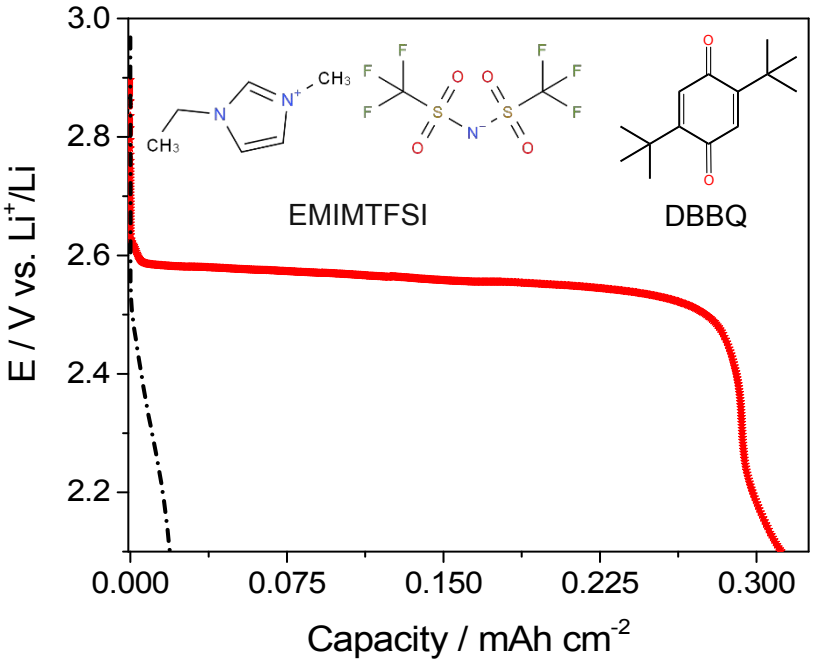

Figure 1. Galvanostatic discharge of Li-O_2 cells with 1 M LiTFSI/EMIMTFSI electrolyte with (red) and without (black) 50 mM DBBQ additive. Both cells were discharged at 0.02 mA/cm^2 (normalized by the geometric area of the electrode).

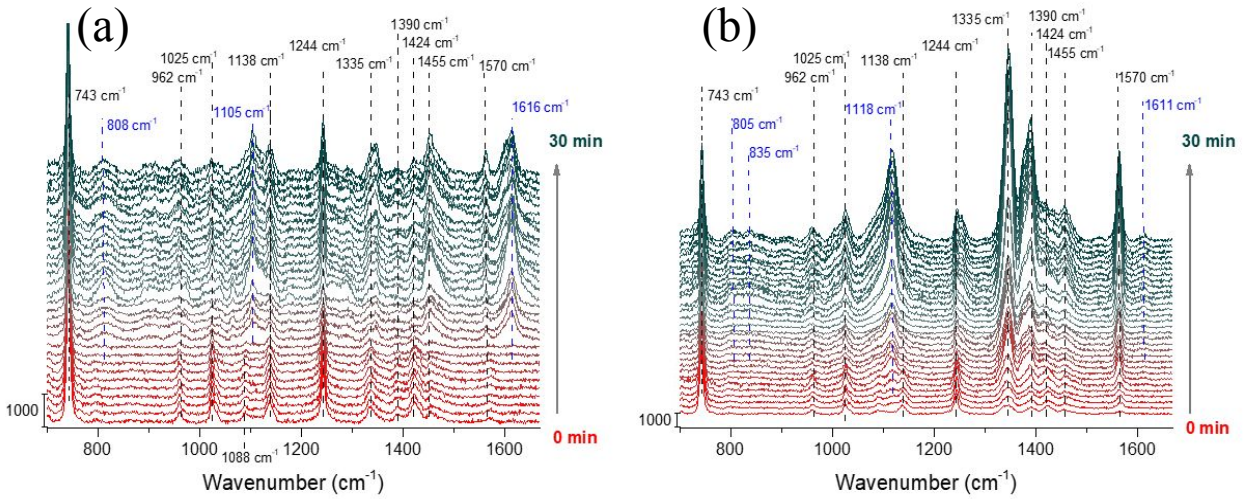

Figure 2. SERS spectra recorded for a SSV gold electrode in oxygenated 0.1 M LiTFSI/EMIMTFSI electrolyte without (a) and with (b) 5 mM DBBQ additive. A reduction current of 0.02 mA/cm^2 was applied to the SSV gold working electrode for 30 minutes and the spectra were recorded in-situ every minute. Black dotted lines show Raman bands corresponding to EMIMTFSI (Table S2) and blue dotted lines corresponds to new bands evolved during ORR.

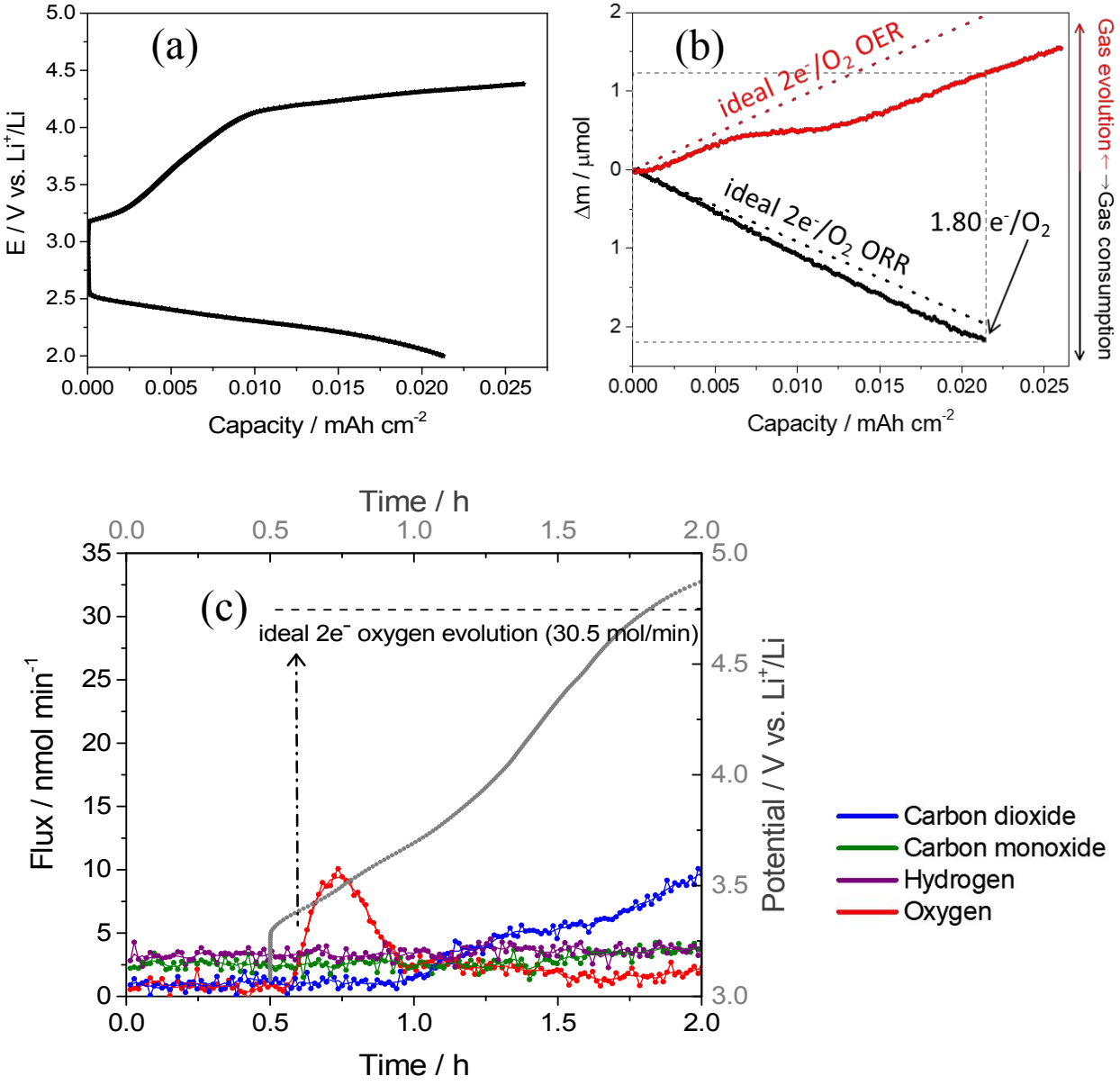

Figure 3. Galvanostatic cycling (a), corresponding gas consumption and evolution analysis obtained from operando pressure measurements (b) and OEMS analysis of gas evolution (c) of Li-O_2 cells with 1 M LiTFSI/EMIMTFSI electrolyte and no additives. Applied current: 0.02 mA/cm^2. The dotted line in Figure 3b shows gas consumption/evolution for an ideal 2-electron ORR/OER. The dashed line in Figure 3c shows the rate of oxygen evolution expected for an

ideal 2-electron OER. Differences in charging profile in Figures 3a,b and 3c reflect cell to cell variability, which is severe due to degradation of EMIMTFSI in the absence of redox mediators.

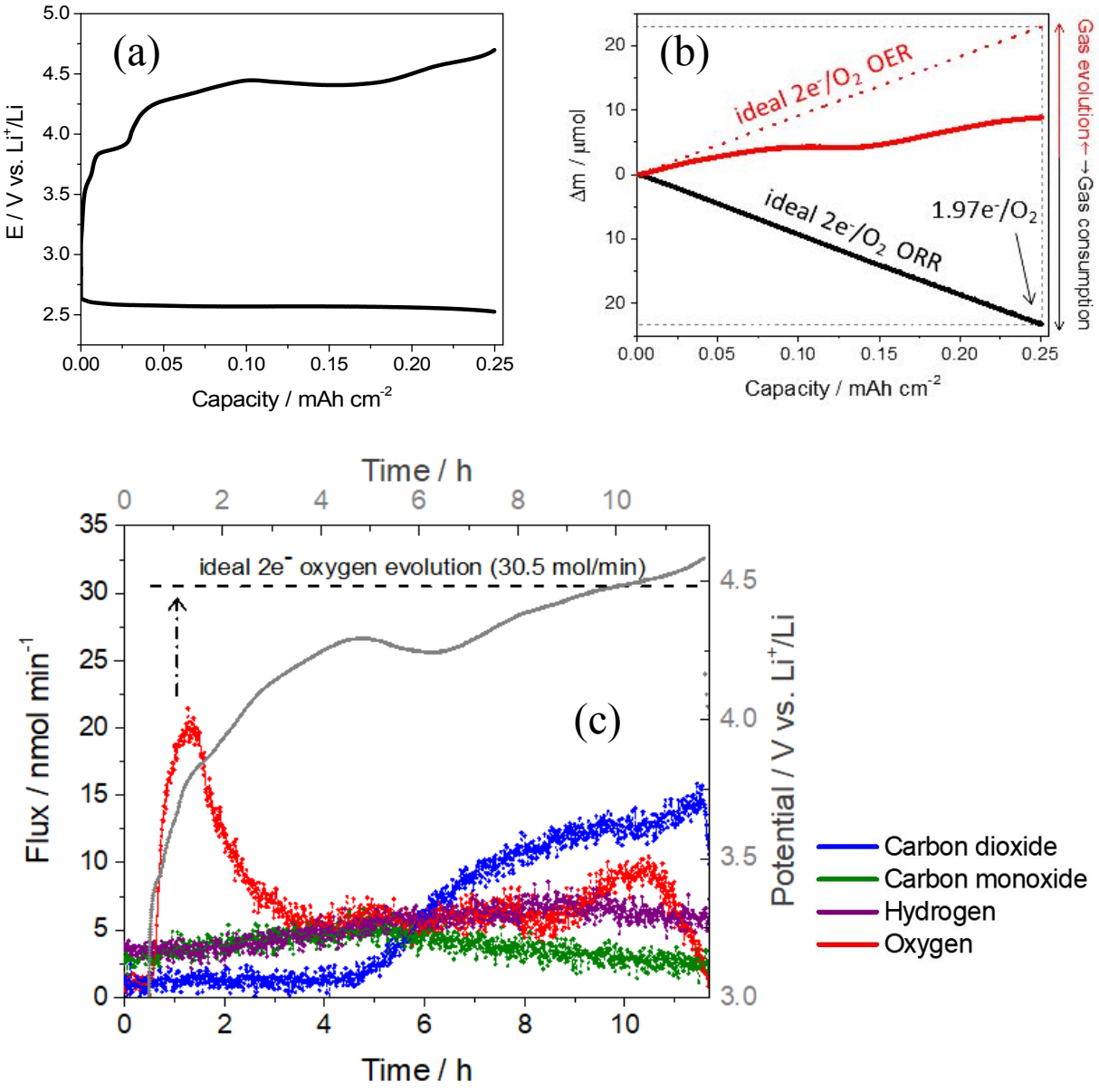

Figure 4. As in Figure 3 but with 1 M LiTFSI/EMIMTFSI electrolyte containing 50 mM DBBQ. Note that, since the experimental gas consumption is in good agreement with the simulated dotted line, the dotted line for ideal 2e-ORR is hidden under the experimental solid line in Figure 4(b).

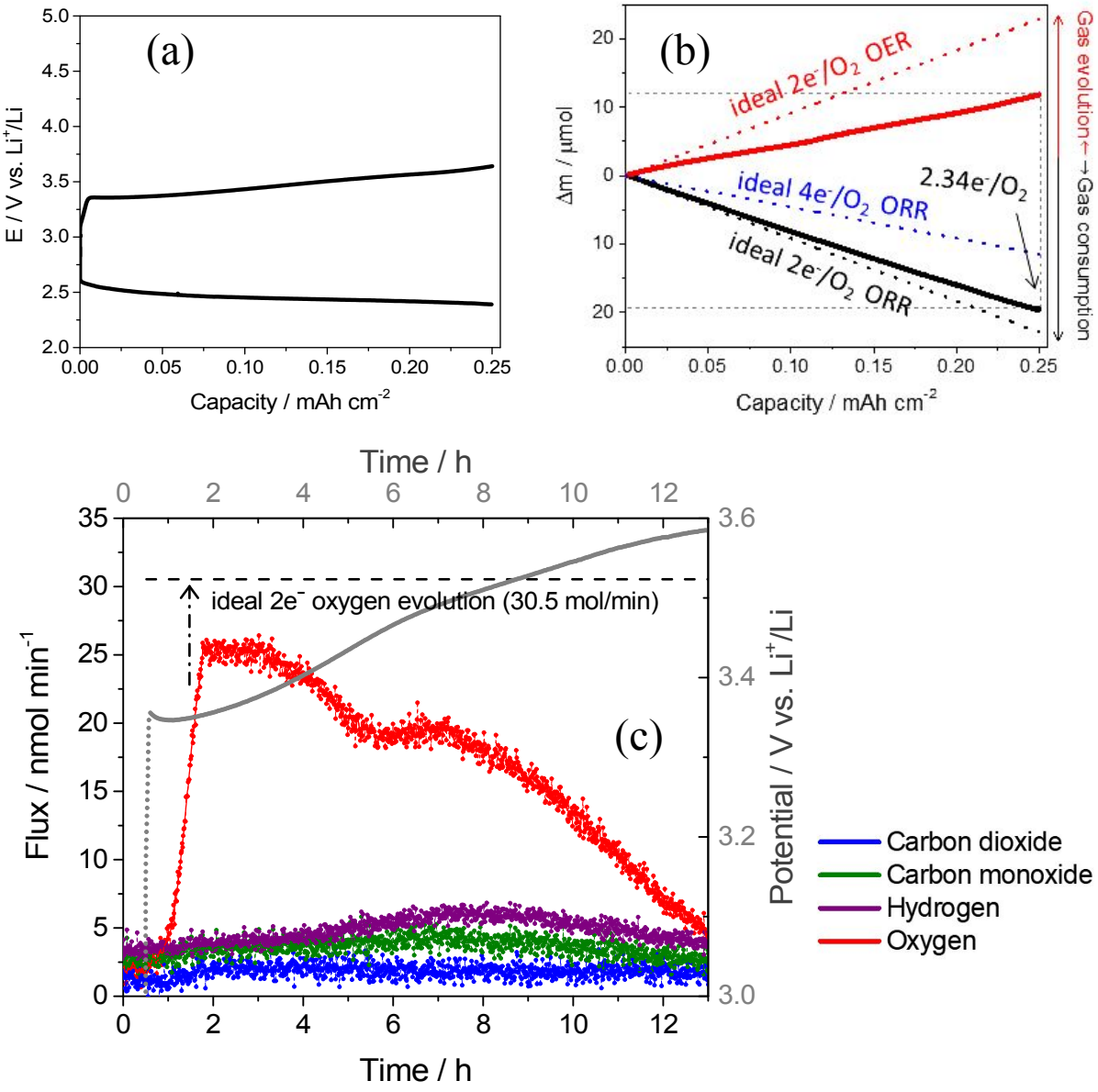

Figure 5. As in Figure 3 but with 1 M LiTFSI/EMIMTFSI electrolyte containing dual mediators 50 mM DBBQ and 50 mM iodide.

REFERENCES

(1) Peng, Z.; Freunberger, S. A.; Chen, Y.; Bruce, P. G. A Reversible and Higher-Rate Li-O_2 Battery. *Science* **2012**, *337*, 563–566.

(2) Scrosati, B., Abraham, K. M., Van Schalkwijk, W., Hassoun, J. Lithium Batteries−Advanced Technologies and Applications; John Wiley & Sons, Inc. New York, **2013**.

(3) Luntz, A. C.; McCloskey, B. D. Nonaqueous Li–Air Batteries: A Status Report. *Chem. Rev.* **2014**, *114*, 11721–11750.

(4) Kundu, D.; Black, R.; Adams, B.; Nazar, L. F. A Highly Active Low Voltage Redox Mediator for Enhanced Rechargeability of Lithium-Oxygen Batteries. *ACS Cent. Sci.* **2015**, *1*, 510–515.

(5) Liu, T.; Leskes, M.; Yu, W.; Moore, A. J.; Zhou, L.; Bayley, P. M.; Kim, G.; Grey, C. P. Cycling Li-O2 Batteries via LiOH Formation and Decomposition. *Science* **2015**, *350*, 530–533.

(6) Aurbach, D.; McCloskey, B. D.; Nazar, L. F.; Bruce, P. G. Advances in Understanding Mechanisms Underpinning Lithium–Air Batteries. *Nat. Energy* **2016**, *1*, 16128.

(7) Lu, J.; Jung Lee, Y.; Luo, X.; Chun Lau, K.; Asadi, M.; Wang, H.-H.; Brombosz, S.; Wen, J.; Zhai, D.; Chen, Z.; et al. A Lithium–Oxygen Battery Based on Lithium Superoxide. *Nature* **2016**, *529*, 377–382.

(8) Feng, N.; He, P.; Zhou, H. Critical Challenges in Rechargeable Aprotic Li-O_2 Batteries. *Adv. Energy Mater.* **2016**, *6*, 1502303.

(9) Liu, T.; Liu, Z.; Kim, G.; Frith, J. T.; Garcia-Araez, N.; Grey, C. P. Understanding LiOH Chemistry in a Ruthenium-Catalyzed Li-O_2 Battery. *Angew. Chemie Int. Ed.* **2017**, *56*, 16057–16062.

(10) Xia, C.; Kwok, C. Y.; Nazar, L. F. A High-Energy-Density Lithium-Oxygen Battery Based on a Reversible Four-Electron Conversion to Lithium Oxide. *Science* **2018**, *361*, 777–781.

(11) Asadi, M.; Sayahpour, B.; Abbasi, P.; Ngo, A. T.; Karis, K.; Jokisaari, J. R.; Liu, C.; Narayanan, B.; Gerard, M.; Yasaei, P.; et al. A Lithium-Oxygen Battery with a Long Cycle Life in an Air-like Atmosphere. *Nature* **2018**, 555, 502–506.

(12) Abraham, K. M. A Polymer Electrolyte-Based Rechargeable Lithium/Oxygen Battery. *J. Electrochem. Soc.* **1996**, *143*, 1.

(13) Shao, Y.; Park, S.; Xiao, J.; Zhang, J. G.; Wang, Y.; Liu, J. Electrocatalysts for Nonaqueous Lithium-Air Batteries: Status, Challenges, and Perspective. *ACS Catal.* **2012**, *2*, 844–857.

(14) Christensen, J.; Albertus, P.; Sanchez-Carrera, R. S.; Lohmann, T.; Kozinsky, B.; Liedtke, R.; Ahmed, J.; Kojic, A. A Critical Review of Li/Air Batteries. *J. Electrochem. Soc.* **2011**, *159*, R1–R30.

(15) Lu, Y.-C.; Gallant, B. M.; Kwabi, D. G.; Harding, J. R.; Mitchell, R. R.; Whittingham, M. S.; Shao-Horn, Y. Lithium-Oxygen Batteries: Bridging Mechanistic Understanding and Battery Performance. *Energy Env. Sci.* **2013**, *6*, 750–768.

(16) Garcia-Araez, N.; Novák, P. Critical Aspects in the Development of Lithium–Air

Batteries. *J. Solid State Electrochem.* **2013**, *17*, 1793–1807.

(17) Gallagher, K. G.; Goebel, S.; Greszler, T.; Mathias, M.; Oelerich, W.; Eroglu, D.; Srinivasan, V. Quantifying the Promise of Lithium–Air Batteries for Electric Vehicles. *Energy Environ. Sci.* **2014**, *7*, 1555.

(18) Balaish, M.; Kraytsberg, A.; Ein-Eli, Y. A Critical Review on Lithium-Air Battery Electrolytes. *Phys. Chem. Chem. Phys.* **2014**, *16*, 2801–2822.

(19) Abraham, K. M. Prospects and Limits of Energy Storage in Batteries. *J. Phys. Chem. Lett.* **2015**, *6*, 830–844.

(20) Scrosati, B. The Lithium Air Battery: Fundamentals. Edited by Nobiyuki Imanishi, Alan C. Luntz, and Peter G. Bruce. *Angew. Chemie Int. Ed.* **2015**, *54*, 5554–5554.

(21) Grande, L.; Paillard, E.; Hassoun, J.; Park, J.-B.; Lee, Y.-J.; Sun, Y.-K.; Passerini, S.; Scrosati, B. The Lithium/Air Battery: Still an Emerging System or a Practical Reality? *Adv. Mater.* **2015**, *27*, 784–800.

(22) Mahne, N.; Fontaine, O.; Thotiyl, M. O.; Wilkening, M.; Freunberger, S. A. Mechanism and Performance of Lithium–Oxygen Batteries – a Perspective. *Chem. Sci.* **2017**, *8*, 6716–6729.

(23) Freunberger, S. A.; Chen, Y.; Peng, Z.; Griffin, J. M.; Hardwick, L. J.; Bardé, F.; Novák, P.; Bruce, P. G. Reactions in the Rechargeable Lithium–O_2 Battery with Alkyl Carbonate Electrolytes. *J. Am. Chem. Soc.* **2011**, *133*, 8040–8047.

(24) Bryantsev, V. S.; Blanco, M. Computational Study of the Mechanisms of Superoxide-Induced Decomposition of Organic Carbonate-Based Electrolytes. *J. Phys. Chem. Lett.*

2011, 2, 379-383.

(25) Wandt, J.; Jakes, P.; Granwehr, J.; Gasteiger, H. A.; Eichel, R.-A. Singlet Oxygen Formation during the Charging Process of an Aprotic Lithium-Oxygen Battery. *Angew. Chemie Int. Ed.* **2016**, *55*, 6892–6895.

(26) Mahne, N.; Schafzahl, B.; Leypold, C.; Leypold, M.; Grumm, S.; Leitgeb, A.; Strohmeier, G. A.; Wilkening, M.; Fontaine, O.; Kramer, D.; et al. Singlet Oxygen Generation as a Major Cause for Parasitic Reactions during Cycling of Aprotic Lithium–Oxygen Batteries. *Nat. Energy* **2017**, *2*, 17036.

(27) McCloskey, B. D.; Bethune, D. S.; Shelby, R. M.; Mori, T.; Scheffler, R.; Speidel, A.; Sherwood, M.; Luntz, A. C. Limitations in Rechargeability of Li-O $_2$ Batteries and Possible Origins. *J. Phys. Chem. Lett.* **2012**, *3*, 3043–3047.

(28) Adams, B. D.; Black, R.; Williams, Z.; Fernandes, R.; Cuisinier, M.; Berg, E. J.; Novak, P.; Murphy, G. K.; Nazar, L. F. Towards a Stable Organic Electrolyte for the Lithium Oxygen Battery. *Adv. Energy Mater.* **2015**, *5*, 1400867.

(29) Yao, X.; Dong, Q.; Cheng, Q.; Wang, D. Why Do Lithium-Oxygen Batteries Fail: Parasitic Chemical Reactions and Their Synergistic Effect. *Angew. Chemie Int. Ed.* **2016**, *55*, 11344–11353.

(30) Lacey, M. J.; Frith, J. T.; Owen, J. R. A Redox Shuttle to Facilitate Oxygen Reduction in the Lithium Air Battery. *Electrochem. Commun.* **2013**, *26*, 74–76.

(31) Chen, Y.; Freunberger, S. A.; Peng, Z.; Fontaine, O.; Bruce, P. G. Charging a Li–O_2 Battery Using a Redox Mediator. *Nat. Chem.* **2013**, *5*, 489–494.

(32) Matsuda, S.; Hashimoto, K.; Nakanishi, S. Efficient Li_2O_2 Formation via Aprotic Oxygen Reduction Reaction Mediated by Quinone Derivatives. *J. Phys. Chem. C* **2014**, *118*, 18397–18400.

(33) Sun, D.; Shen, Y.; Zhang, W.; Yu, L.; Yi, Z.; Yin, W.; Wang, D. D.; Huang, Y.; Wang, J.; Wang, D. D.; et al. A Solution-Phase Bifunctional Catalyst for Lithium–Oxygen Batteries. *J. Am. Chem. Soc.* **2014**, *136*, 8941–8946.

(34) Johnson, L.; Li, C.; Liu, Z.; Chen, Y.; Freunberger, S. A.; Ashok, P. C.; Praveen, B. B.; Dholakia, K.; Tarascon, J.-M.; Bruce, P. G. The Role of LiO2 Solubility in O2 Reduction in Aprotic Solvents and Its Consequences for Li–O_2 Batteries. *Nat. Chem.* **2014**, *6*, 1091–1099.

(35) Aetukuri, N. B.; McCloskey, B. D.; García, J. M.; Krupp, L. E.; Viswanathan, V.; Luntz, A. C. Solvating Additives Drive Solution-Mediated Electrochemistry and Enhance Toroid Growth in Non-Aqueous Li–O_2 Batteries. *Nat. Chem.* **2015**, *7*, 50–56.

(36) Matsuda, S.; Uosaki, K.; Nakanishi, S. Enhanced Energy Capacity of Lithium-Oxygen Batteries with Ionic Liquid Electrolytes by Addition of Ammonium Ions. *J. Power Sources* **2017**, *356*, 12–17.

(37) Gao, X.; Jovanov, Z. P.; Chen, Y.; Johnson, L. R.; Bruce, P. G. Phenol-Catalyzed Discharge in the Aprotic Lithium-Oxygen Battery. *Angew. Chemie Int. Ed.* **2017**, *56*, 6539–6543.

(38) Liu, T.; Frith, J. T.; Kim, G.; Kerber, R. N.; Dubouis, N.; Shao, Y.; Liu, Z.; Magusin, P. C. M. M.; Casford, M. T. L.; Garcia-Araez, N.; et al. The Effect of Water on Quinone

Redox Mediators in Nonaqueous Li-O $_2$ Batteries. *J. Am. Chem. Soc.* **2018**, *140*, 1428–1437.

(39) Homewood, T.; Frith, J. T.; Vivek, J. P.; Casañ-Pastor, N.; Tonti, D.; Owen, J. R.; Garcia-Araez, N. Using Polyoxometalates to Enhance the Capacity of Lithium-Oxygen Batteries. *Chem. Commun.* **2018**, *54*, 9599–9602.

(40) Yang, L.; Frith, J. T.; Garcia-Araez, N.; Owen, J. R. A New Method to Prevent Degradation of Lithium–Oxygen Batteries: Reduction of Superoxide by Viologen. *Chem. Commun.* **2015**, *51*, 1705–1708.

(41) Liang, Z.; Lu, Y.-C. C. Critical Role of Redox Mediator in Suppressing Charging Instabilities of Lithium-Oxygen Batteries. *J. Am. Chem. Soc.* **2016**, *138*, 7574–7583.

(42) Garcia, B.; Lavallée, S.; Perron, G.; Michot, C.; Armand, M. Room Temperature Molten Salts as Lithium Battery Electrolyte. *Electrochim. Acta* **2004**, *49*, 4583–4588.

(43) MacFarlane, D. R.; Forsyth, M.; Howlett, P. C.; Pringle, J. M.; Sun, J.; Annat, G.; Neil, W.; Izgorodina, E. I. Ionic Liquids in Electrochemical Devices and Processes: Managing Interfacial Electrochemistry. *Acc. Chem. Res.* **2007**, *40*, 1165–1173.

(44) Armand, M.; Endres, F.; MacFarlane, D. R.; Ohno, H.; Scrosati, B. Ionic-Liquid Materials for the Electrochemical Challenges of the Future. *Nat. Mater.* **2009**, *8*, 621–629.

(45) Lewandowski, A.; Świderska-Mocek, A. Ionic Liquids as Electrolytes for Li-Ion Batteries—An Overview of Electrochemical Studies. *J. Power Sources* **2009**, *194*, 601–609.

(46) MacFarlane, D. R.; Tachikawa, N.; Forsyth, M.; Pringle, J. M.; Howlett, P. C.; Elliott, G.

D.; Davis, J. H.; Watanabe, M.; Simon, P.; Angell, C. A. Energy Applications of Ionic Liquids. *Energy Environ. Sci.* **2014**, *7*, 232–250.

(47) Islam, M. M.; Imase, T.; Okajima, T.; Takahashi, M.; Niikura, Y.; Kawashima, N.; Nakamura, Y.; Ohsaka, T. Stability of Superoxide Ion in Imidazolium Cation-Based Room-Temperature Ionic Liquids. *J. Phys. Chem. A* **2009**, *113*, 912–916.

(48) Frith, J. T.; Russell, A. E.; Garcia-Araez, N.; Owen, J. R. An In-Situ Raman Study of the Oxygen Reduction Reaction in Ionic Liquids. *Electrochem. Commun.* **2014**, *46*, 33–35.

(49) Yeager, E. Electrocatalysts for O_2 Reduction. *Electrochim. Acta* **1984**, *29*, 1527–1537.

(50) Barnes, A. S.; Rogers, E. I.; Streeter, I.; Aldous, L.; Hardacre, C.; Wildgoose, G. G.; Compton, R. G. Unusual Voltammetry of the Reduction of O_2 in $[C_4dmim][N(Tf)_2]$ Reveals a Strong Interaction of $O_2^{\bullet-}$ with the $[C_4dmim]^+$ Cation. *J. Phys. Chem. C* **2008**, *112*, 13709–13715.

(51) Bonhôte, P.; Dias, A.P.; Papageorgiou, N.; Kalyanasundaram, K.; Grätzel, M. Hydrophobic, Highly Conductive Ambient-Temperature Molten Salts. *Inorg. Chem.* **1996**, *35*, 1168–1178.

(52) Sun, J.; MacFarlane, D. R.; Forsyth, M. Synthesis and Properties of Ambient Temperature Molten Salts Based on the Quaternary Ammonium Ion. *Ionics* **1997**, *3*, 356–362.

(53) Sun, J.; Forsyth, M.; MacFarlane, D. R. Room-Temperature Molten Salts Based on the Quaternary Ammonium Ion. *J. Phys. Chem. B* **1998**, 102, 8858-8864.

(54) Gao, X.; Chen, Y.; Johnson, L.; Bruce, P. G. Promoting Solution Phase Discharge in Li–O2 Batteries Containing Weakly Solvating Electrolyte Solutions. *Nat. Mater.* **2016**, *15*,

882–888.

(55) Mahajan, S.; Baumberg, J. J.; Russell, A. E.; Bartlett, P. N. Reproducible SERRS from Structured Gold Surfaces. *Phys. Chem. Chem. Phys.* **2007**, *9*, 6016.

(56) Abdelsalam, M. E.; Bartlett, P. N.; Baumberg, J. J.; Cintra, S.; Kelf, T. A.; Russell, A. E. Electrochemical SERS at a Structured Gold Surface. *Electrochem. Commun.* **2005**, *7*, 740–744.

(57) Buzzeo, M. C.; Klymenko, O. V.; Wadhawan, J. D.; Hardacre, C.; Seddon, K. R.; Compton, R. G. Voltammetry of Oxygen in the Room-Temperature Ionic Liquids 1-Ethyl-3-Methylimidazolium Bis((Trifluoromethyl)Sulfonyl)Imide and Hexyltriethylammonium Bis((Trifluoromethyl)Sulfonyl)Imide: One-Electron Reduction to Form Superoxide. Steady-State and Transien. *J. Phys. Chem. A* **2003**, *107*, 8872–8878.

(58) Zhang, D.; Okajima, T.; Matsumoto, F.; Ohsaka, T. Electroreduction of Dioxygen in 1-n-Alkyl-3-Methylimidazolium Tetrafluoroborate Room-Temperature Ionic Liquids. *J. Electrochem. Soc.* **2004**, *151*, D31.

(59) Radjenovic, P. M.; Hardwick, L. J. Time-Resolved SERS Study of the Oxygen Reduction Reaction in Ionic Liquid Electrolytes for Non-Aqueous Lithium–Oxygen Cells. *Faraday Discuss.* **2018**, *206*, 379–392.

(60) Li, C.; Fontaine, O.; Freunberger, S. A.; Johnson, L.; Grugeon, S.; Bruce, P. G.; Armand, M.; Laruelle, S.; Bruce, P. G.; Armand, M. Aprotic Li − O 2 Battery : Influence of Complexing Agents on Oxygen Reduction in an Aprotic Solvent. *J. Phys. Chem. C* **2014**, *118*, 3393–3401.

(61) Li, F.; Wu, S.; Li, D.; Zhang, T.; He, P.; Yamada, A.; Zhou, H. The Water Catalysis at Oxygen Cathodes of Lithium-Oxygen Cells. *Nat. Commun.* **2015**, *6*, 1–7.

(62) Kwak, W.-J.; Hirshberg, D.; Sharon, D.; Shin, H.-J.; Afri, M.; Park, J.-B.; Garsuch, A.; Chesneau, F. F.; Frimer, A. A.; Aurbach, D.; et al. Understanding the Behavior of Li–Oxygen Cells Containing LiI. *J. Mater. Chem. A* **2015**, *3*, 8855–8864.

(63) Burke, C. M.; Black, R.; Kochetkov, I. R.; Giordani, V.; Addison, D.; Nazar, L. F.; McCloskey, B. D. Implications of 4 e ⁻ Oxygen Reduction via Iodide Redox Mediation in Li–O_2 Batteries. *ACS Energy Lett.* **2016**, *1*, 747–756.

(64) Qiao, Y.; Wu, S.; Sun, Y.; Guo, S.; Yi, J.; He, P.; Zhou, H. Unraveling the Complex Role of Iodide Additives in Li–O $_2$ Batteries. *ACS Energy Lett.* **2017**, *2*, 1869–1878.

(65) Zhu, Y. G.; Liu, Q.; Rong, Y.; Chen, H.; Yang, J.; Jia, C.; Yu, L. J.; Karton, A.; Ren, Y.; Xu, X.; et al. Proton Enhanced Dynamic Battery Chemistry for Aprotic Lithium-Oxygen Batteries. *Nat. Commun.* **2017**, *8*, 4–11.

(66) Li, Z.; Ganapathy, S.; Xu, Y.; Heringa, J. R.; Zhu, Q.; Chen, W.; Wagemaker, M. Understanding the Electrochemical Formation and Decomposition of Li_2O_2 and LiOH with *Operando* X-Ray Diffraction. *Chem. Mater.* **2017**, *29*, 1577–1586.

(67) Liu, T.; Kim, G.; Jónsson, E.; Castillo-Martinez, E.; Temprano, I.; Shao, Y.; Carretero-González, J.; Kerber, R. N.; Grey, C. P. Understanding LiOH Formation in a Li-O_2 Battery with LiI and H $_2$ O Additives. *ACS Catal.* **2019**, *9*, 66–77.

(68) Meini, S.; Solchenbach, S.; Piana, M.; Gasteiger, H. A. The Role of Electrolyte Solvent Stability and Electrolyte Impurities in the Electrooxidation of Li_2O_2 in Li-O_2 Batteries. *J.*

Electrochem. Soc. **2014**, *161*, A1306–A1314.

(69) Zhu, Y. G.; Jia, C.; Yang, J.; Pan, F.; Huang, Q.; Wang, Q. Dual Redox Catalysts for Oxygen Reduction and Evolution Reactions: Towards a Redox Flow Li–O_2 Battery. *Chem. Commun.* **2015**, *51*, 9451–9454.

(70) Zhu, Y. G.; Wang, X.; Jia, C.; Yang, J.; Wang, Q. Redox-Mediated ORR and OER Reactions: Redox Flow Lithium Oxygen Batteries Enabled with a Pair of Soluble Redox Catalysts. *ACS Catal.* **2016**, *6*, 6191–6197.

(71) Gao, X.; Chen, Y.; Johnson, L. R.; Jovanov, Z. P.; Bruce, P. G. A Rechargeable Lithium–Oxygen Battery with Dual Mediators Stabilizing the Carbon Cathode. *Nat. Energy* **2017**, *2*, 17118.

(72) Zhu, Y. G.; Goh, F. W. T.; Yan, R.; Wu, S.; Adams, S.; Wang, Q. Synergistic Oxygen Reduction of Dual Redox Catalysts Boosting the Power of Lithium–Air Battery. *Phys. Chem. Chem. Phys.* **2018**, *20*, 27930–27936.

TOC Graphic

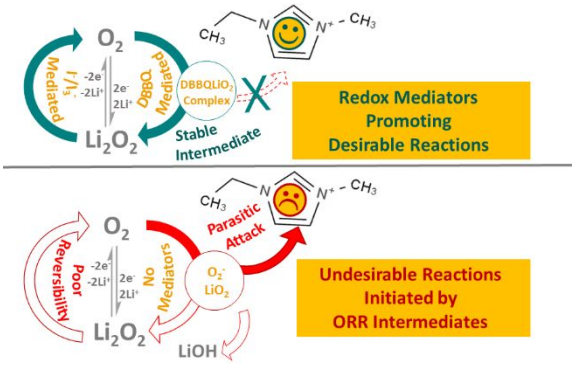
O2
-2e-
-2Li+
2e-
2Li+
I-/I3- Mediated
DBBQ Mediated
Li2O2
DBBQLiO2 Complex
Stable Intermediate
Redox Mediators Promoting Desirable Reactions
Parasitic Attack
Poor Reversibility
No Mediators
O2-
LiO2
Li2O2
LiOH
Undesirable Reactions Initiated by ORR Intermediates